

# Break-up testing of waste-form materials

M. P. METCALFE<sup>1,\*</sup>, W. KOCH<sup>2</sup> AND G. TURNER<sup>3</sup>

<sup>1</sup> National Nuclear Laboratory, Stonehouse Park, Bristol Road, Stonehouse GL10 3UT, UK

<sup>2</sup> Fraunhofer Institut, Nikolai-Fuchs Strasse 1, 30625 Hannover, Germany

<sup>3</sup> Nuclear Decommissioning Authority, Curie Avenue, Harwell Science and Innovation Campus, Didcot OX11 0RH, UK

[Received 18 December 2011; Accepted 29 March 2012; Associate Editor: Nicholas Evans]

## ABSTRACT

The Nuclear Decommissioning Authority (NDA) is developing a safety case for the long-term management of higher activity wastes. This includes safety assessments of transport to and operations at the repository. One of the main faults and hazards to be considered is waste package response to impact accidents.

The criteria of impact performance for waste packages are based upon activity release of particulates generated from the break up of the waste form during impact. The NDA approach to impact performance is based upon waste package response from finite element modelling in combination with break-up tests.

Previous break up research commissioned by the NDA has concentrated on commercial graphite and glass samples. These extended studies, undertaken by the National Nuclear Laboratory in collaboration with the Department of Aerosol Technology of the Fraunhofer Institute of Toxicology and Experimental Medicine, provide break-up data specific to nuclear facilities and waste materials. These include archived unirradiated graphite used to construct Magnox reactor cores and reflectors, simulant high level waste glass, selected grout formulations and selected metal-in-grout formulations.

**KEYWORDS:** break-up testing, graphite, high level waste glass, impact testing, radioactive waste.

## Introduction

FINITE ELEMENT (FE) analysis can be used in the prediction of waste package and waste-form behaviour in impact scenarios. Coupled with information gained from small-scale test data, predictions of the amount of activity release from a waste package can be made. Data from small scale break-up tests which completely characterize the waste-form for modelling purposes include airborne release fractions and a particle size distribution function.

The objective of this work is to provide new break-up data on samples of graphite (waste from decommissioned nuclear plant), glass (waste immobilization matrix) and cemented materials/

grout (packaging and encapsulation material). The parameter of interest is the amount and the aerodynamic size distribution of released airborne material [ $<100 \mu\text{m}$  aerodynamic equivalent diameter (AED)] generated during fragmentation of small-scale specimens under transient mechanical energy inputs of different magnitude. The specific energy imposed on the test specimens covers a range representing local energy densities of large scale specimens under accident scenarios, represented by impact velocities varying between 13 and  $70 \text{ m s}^{-1}$ .

## Test materials

Two grades of unirradiated graphite were selected for testing, representing the most extensively used graphite across the UK Magnox nuclear reactor fleet: pile grade A (PGA) and pile grade B (PGB)

\* E-mail: martin.p.metcalfe@nnl.co.uk

DOI: 10.1180/minmag.2012.076.8.13

graphites. The impact test facility was unable to accommodate irradiated material and the implications of this on the validity of the test data are discussed below. The material was sourced from an inactive graphite archive maintained by the NDA.

Highly active liquid (HAL) waste, which consists of a concentrated nitric acid solution of fission products, corrosion products and process additives from the reprocessing of spent nuclear fuel, is immobilized in stable glass monoliths in the UK by the Waste Vitrification Plant (WVP) at Sellafield. The WVP product is largely a homogeneous material with the highly active waste fully dispersed and chemically bound and immobilized within the glass matrix on an atomic scale. There is, however, always a small amount (<2 vol.%) of encapsulated crystalline material present in the final WVP product due to some species in the HAL being insoluble in the glass. The predominant crystalline phases that form are platinoids, evenly distributed throughout the glass monolith with no evidence for settling during cooling. The presence of these crystalline inclusions may have a noticeable affect on properties relating to the impact testing, so representative concentrations of platinoids and spinels in the glass samples have been included during fabrication of simulant composition test specimens. The inactive glass specimens cover glass produced from Magnox reprocessing and glass produced when Magnox and THORP liquors are blended. In addition, base glass specimens were included in the test programme, this being a mixed alkali borosilicate ('MW') glass into which calcined waste oxides are dissolved. Although high level waste (HLW) glass is subject to both significant radiation fields and elevated temperatures for several years, it is currently thought that properties are not altered significantly. There may be extra cracking within the matrix, but testing of freshly prepared material was judged to be adequately representative.

Intermediate-level waste is encapsulated within grout inside stainless steel containers. The variability of the type of waste has led to the use of different grouts dependant upon their properties. The formulations selected for testing consisted of mixes of pulverised fuel ash (PFA) with ordinary Portland cement (OPC) and blast furnace slag (BFS) with OPC. The actual formulations were based upon grout formulation envelopes developed for the Magnox Encapsulation Plant at Sellafield. In addition, selected formulations were prepared with metal grit loadings to represent waste containers containing metal. This metal can vary significantly in surface area and volume and two grit sizes were chosen to build on previous studies (Nolte, 2005). Test specimens were made from freshly prepared material on the basis that irradiation effects would be insignificant over timescales associated with waste container preparation and movements to a storage facility. The selection of test materials is summarized in Table 1.

### Test methodology

The basic quantity of interest for modelling studies is the mass and size distribution function of the airborne fragments. This is conveniently described by the cumulative mass fraction,  $Q_3(d_{ae})$ , as a function of the aerodynamic diameter,  $d_{ae}$ :

$$Q_3(d_{ae}) = \frac{m(d_{ae})}{M_s} \quad (1)$$

where  $m(d_{ae})$  is the mass of all particles released in the size range smaller than  $d_{ae}$ , and  $M_s$  is the mass of the test specimen. The values of this function at 100  $\mu\text{m}$  are shown in equation 2:

$$\eta_{100} = Q_3(100 \mu\text{m}) \quad (2)$$

TABLE 1. Summary of materials selected for impact testing.

Material type	Formulations
Glass	MW base glass, Magnox glass with 32% waste oxide, blend glass with 28% waste oxide and platinoids
Graphite	Unirradiated PGA and PGB graphite
Grout	BFS/OPC and PFA/OPC formulations with a range of water to solids ratios
Grit in grout	PFA/OPC formulation with two metal grit sizes and a range of grit loadings

Values of  $\eta_{100}$  are of particular interest as they represent the total airborne release fraction smaller than 100  $\mu\text{m}$  and the fraction being able to enter the human respiratory system. The size fraction  $<10 \mu\text{m}$  is considered to be accessible to the lungs. It has shown in previous experiments (for example, Madler, 1999) that fragmentation is determined by the specific energy input,  $W_m$ , into the specimen and that the formation of dust is related to  $W_m$  as follows:

$$\eta_{100} = A + bW_m \quad (3)$$

Another outcome of such experimental work, as well as theoretical evidence (Grady, 2008), concerns the particle size distribution function. It has been shown that there is no characteristic fragment size in the fragmentation process of brittle material and that fragment size exhibits self-similarity. Consequently the size distribution function is characterized by a power law function:

$$Q_3(d_{ae}) \propto d_{ae}^k \quad (4)$$

This implies that if the cumulative mass distribution is known for one value of the aerodynamic diameter, for example at 100  $\mu\text{m}$ , all other values can be calculated using equation 4.

If the parameters,  $A$ ,  $b$  and  $k$  are known for the waste-form, based on break-up tests, the dust formation characteristics of this material are completely described.

It is not feasible to carry out impact tests with large package sizes to measure the dust release directly. Instead dust release is estimated by performing a theoretical analysis of the distribution of energy inside the package using FE codes and using equations 3 and 4 to calculate the amount of airborne dust ( $<100 \mu\text{m}$ ) and the respirable fraction ( $<10 \mu\text{m}$ ) that can be generated locally and potentially be released.

**Test rig and specimens**

The test rig for small scale tests developed at Fraunhofer ITEM consists of a pneumatic gun for accelerating test specimens with a maximum diameter of 43 mm to velocities up to 100  $\text{m s}^{-1}$ , a hard impact surface (unyielding iron plate), and an aerodynamic classification unit (Fig. 1). In the classification unit, all airborne particles with aerodynamic diameters smaller than 100  $\mu\text{m}$  originating from the fragmentation process are separated from the larger fragments in a vertical

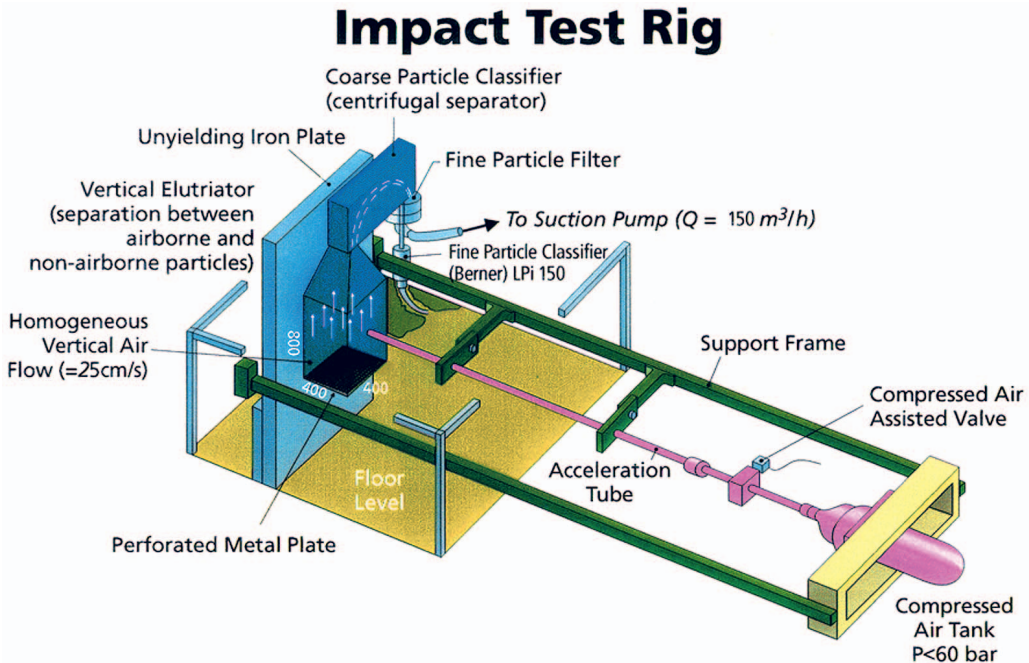


FIG. 1. Fraunhofer ITEM test rig for small-scale experiments on the release fractions of brittle material after mechanical energy impact.

elutriator. The entire airborne fraction is subsequently classified in three size intervals in the size range between 20 and 100  $\mu\text{m}$  aerodynamic equivalent diameter (AED) and five size intervals below 20  $\mu\text{m}$ . This is achieved by using a combination of a coarse particle classifier (centrifugal separator) and a fine particle classifier, respectively.

The air reservoir has a volume of 20 litres and can be pressurized up to 200 bar. The compressed air can be released promptly by a quick release valve with a large effective cross-sectional area. The release valve is directly connected to the air tank on one side and to the acceleration tube at the other side. The valve is activated electrically and is opened via pressurized air (>180 bar). After the filling process, the gun can be electrically activated remotely.

The velocity of the test specimen is measured at the outlet of the acceleration tube. The time of flight between two light beams interrupted by the passage of the front end of the specimen is measured using a counter. An oscilloscope is used to check the entire output signal. The two light

beams are oriented perpendicular to each other. The time resolution of the measuring device is better than 25  $\mu\text{s}$ .

The unyielding target is mounted upright on the concrete base floor of the laboratory. The specimen does not impact directly on this plate but on a replaceable smaller square. This protects the main plate against undue damage and provides flexibility to change the (material) properties of the impact surface and if required the angle of impact.

The standard test specimen geometry was a cylinder 30 mm in diameter and 50 mm in length. PGA graphite specimens were prepared such that the cylinder axis was either parallel or perpendicular to the material extrusion direction. The PGB graphite specimens could only be prepared in a smaller size and a bridging experiment was included to relate PGA and PGB impact behaviour.

All tests were monitored by a high speed video camera. Figure 2 shows a sequence of three frames taken at three time points: before the impact, at the moment of impact and after

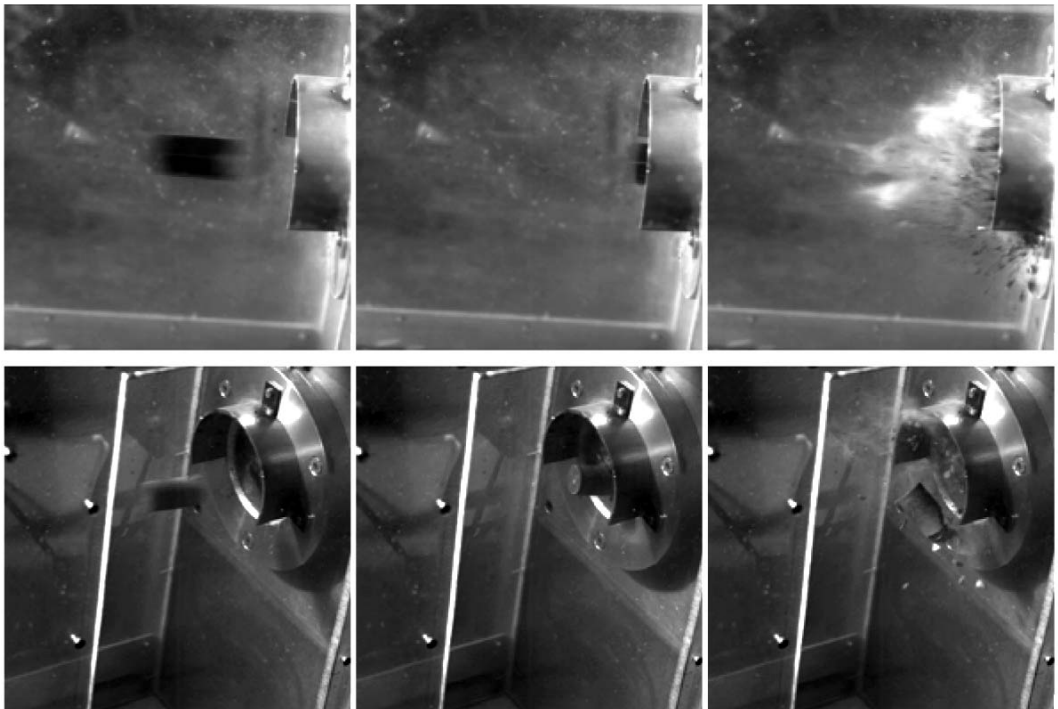


FIG. 2. High speed video frame sequence of two valid impact tests: glass specimen at impact speed of  $60 \text{ m s}^{-1}$  (top images); grit in grout specimen at impact speed of  $28 \text{ m s}^{-1}$  (bottom images).

fragmentation. Tests were considered to be valid when the specimen was not broken apart before the impact.

## Test results and discussion

### Airborne release fraction

The airborne release fraction,  $\eta_{100}$ , was measured for all material types and plotted as a function of the specific energy input. A linear regression was performed for each specimen type to determine the parameters  $A$  and  $b$  in equation 3, the errors in  $A$  and  $b$  and the correlation coefficient. The slope of the plot ( $b$ ) of airborne release fraction versus specific energy input is termed the ‘dustiness’ of the material or its dispersion propensity. For each specimen type, the relative standard error (the standard error divided by the mean and expressed as a either a percentage or a fraction) in the slope,  $b$ , and the Pearson regression coefficient,  $R^2$ , were checked for compliance against acceptance criteria. Tests results for a specimen type were deemed compliant if  $\Delta b/b < 0.15$  and  $R^2 > 0.9$  (approximately 90% of the variation in the response variable explained by the explanatory variable, the remaining 10% explained by unknown inherent variability).

For most of the specimen types, the acceptance criteria were met with five impact tests, where the specific energy input was distributed evenly over the intended range. In the case of the small graphite specimens, the criteria were not met due to the relatively small amounts of dust formed on impact. Increasing the number of tests was not expected to eliminate scatter. In the case of some of the grout specimens, where the criteria were not met, the fits to the test data did not indicate any obvious relationship between dust formation and grout formulation, so there were no perceived benefits from additional testing.

The mean  $A$  and  $b$  values (and their errors) from the regression fits for each of the five

material types are summarized in Table 2. The underlying data for grit in grout are presented in Fig. 3, where the solid line is the regression fit, the error  $\Delta A$  is shown by the upper and lower points on the  $y$  axis and error  $\Delta b$  is shown by the broken lines.

For the offset,  $A$ , there is a significant difference between the glass specimens (offset of 0.001) compared with a value closer to zero for the other three material groups. The reason for the high offset for the glass materials could be that glass shows fragmentation only above a threshold value for the specific energy input, as has been reported for Pyrex glass (Nolte, 2006). The scatter associated with this fitting parameter is quite high due to break-up statistics at low impact energies and experimental limitations for low dust emissions. Of the material types tested, the small graphite specimens gave the largest scatter in airborne release fraction data. This is attributed to, among other factors, measurement errors arising from the small amount of dust collected for such low specimen masses.

The  $b$ -values for glass show no significant difference between the three selected types. Graphite samples with their cylinder axis parallel and perpendicular to the extrusion direction of the material do not differ either. Their  $b$ -values are slightly below those of the glass specimens. However, it is important to note that specimens may rotate when leaving the acceleration tube and, therefore, the angle between the extrusion direction and the impact plate is not well defined. Although this aspect of the experiment design may not have achieved the intended objective (quantification of differences in impact behaviour parallel and perpendicular to extrusion direction), a useful conclusion can be reached. If orientation relative to extrusion at impact was important, this would be reflected in the level of scatter in the data. Despite the observed rotation of specimens and the resulting random impact angles of this

TABLE 2. The mean regression parameter values and their errors for the five different groups of material tested.

	$A$	$\Delta A$	$b$ (kg J <sup>-1</sup> )	$\Delta b$ (kg J <sup>-1</sup> )
Glass	$1.06 \times 10^{-3}$	$5.43 \times 10^{-4}$	$3.88 \times 10^{-6}$	$2.62 \times 10^{-7}$
Graphite	$-2.69 \times 10^{-4}$	$2.50 \times 10^{-4}$	$2.72 \times 10^{-6}$	$9.19 \times 10^{-8}$
Grit in grout	$-2.63 \times 10^{-4}$	$2.68 \times 10^{-4}$	$4.42 \times 10^{-6}$	$8.62 \times 10^{-7}$
PFA/OPC	$-1.15 \times 10^{-4}$	$3.33 \times 10^{-4}$	$3.76 \times 10^{-6}$	$3.97 \times 10^{-7}$
BFS/OPC	$7.46 \times 10^{-5}$	$1.35 \times 10^{-4}$	$3.77 \times 10^{-6}$	$5.83 \times 10^{-7}$

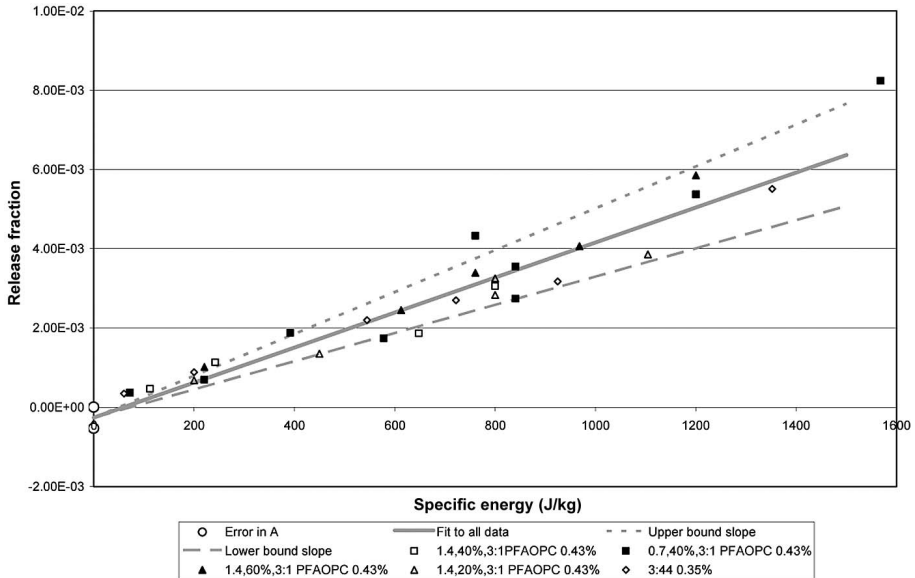


FIG. 3. Summary of airborne release fraction data for grit in grout.

orthotropic material, the data show relatively little scatter when compared with that for isotropic materials. It must therefore be concluded that impact relative to extrusion direction does not have any significant effect upon dust production from graphite. Also, within experimental error, PGA and PGB graphites behave in the same way in terms of dust formation. For the formulations tested, grout composition does not seem to influence the propensity for dispersion. For the grit in grout specimens, there is an increase in dustiness with increasing amount of metal grit surface area mixed into the grout. Overall, the numerical values of *b* vary less than a factor of 2 for all materials tested. It was observed that when the dimension of the graphite test specimen was reduced, there was increased scatter in the data and a trend to higher dust production. This is consistent with previous investigations of glass, ceramics, cement and concrete (for example, Nolte, 2006) that show smaller specimens produce more dust than larger ones. On average, the *b* value for graphite seems to be significantly lower than the value for the other materials as illustrated in Fig. 4.

For glass, threshold values of the specific energy below which no break-up occurs could not be determined using the limited data set available for low impact energies. In this case,

threshold values would be better determined in drop tests, where low energy values can be set with more precision. In terms of data for modelling impact behaviour, linear regression fits for the glass specimens should be used for impact energies above 250 J kg<sup>-1</sup>. At impact energies below this value, a constant value of 2.0 × 10<sup>-3</sup> should be used for η<sub>100</sub> to bound airborne release behaviour. For all other materials, a threshold value for specific energy (below which no break-up occurs) is not recommended. Instead, an airborne dust release should be assumed, even at very low energy input. For the linear regression parameter, *b*, conservative single values of 5.0 × 10<sup>-6</sup> kg J<sup>-1</sup> for glass and grout and 3.0 × 10<sup>-6</sup> kg J<sup>-1</sup> for graphite are proposed.

#### Particle size distribution function

The size distribution data (cumulative mass fraction) for each group of samples tested can be characterized by a power law function (equation 4) which can be written:

$$\frac{Q_3(d_{ae})}{\eta_{100}} = Kd_{ae}^\kappa \quad (5)$$

where *K* is a fitting constant and κ is the size distribution exponent. The existence of scaling



## BREAK-UP TESTING OF WASTE-FORM MATERIALS

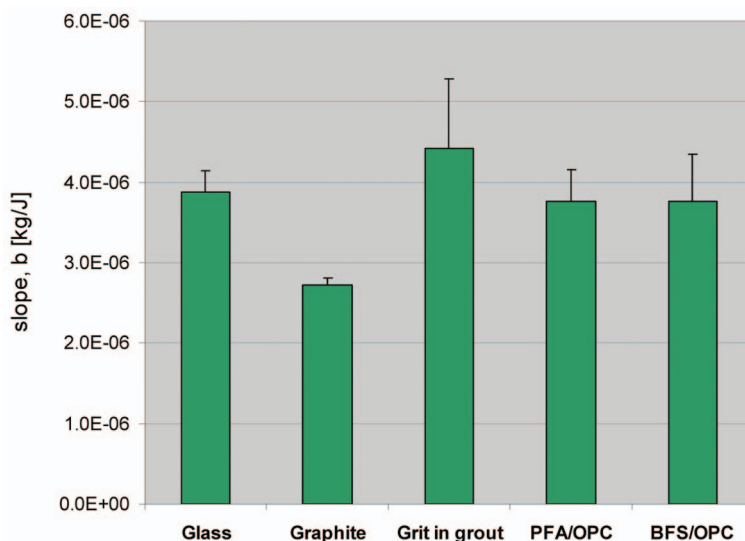


FIG. 4. The value of the slope of the regression line (equation 3) for the five different groups of material tested.

laws for the fragment size distribution has been widely reported both generally (Oddershede *et al.*, 1993; Meibom and Baslev, 1996) and specifically in tests carried out with brittle materials using the same impact test rig as that employed here (Lange *et al.*, 2003, 2007; Madler, 1999).

Mean values for the size distribution component,  $\kappa$ , for each material group tested here are summarized in Table 3. In previous studies (Nolte, 2006), the size distribution exponent for a wide range of materials (including glass, cement and concrete) was found to have values between 0.8 and 1.2. From the test work reported here, values vary between 0.47 and 1.03. In the case of graphite, the value is close to unity.

The value of  $\kappa$  can be assessed more accurately by extending the particle size range to larger

fragment sizes ( $>100 \mu\text{m}$ ). Due to the low mass loadings on the impactor stages for fine particles ( $<10 \mu\text{m}$ ) and larger errors in their detection, it is better to evaluate the size distribution component by combining masses to one single value over this range. This demonstrates that the overall uncertainty of the  $\kappa$ -value can be quite large although the error in  $\kappa$  based on the regression is relatively small.

For regulatory purposes, the respirable fraction ( $<10 \mu\text{m}$ ) is of importance and mean values of this fraction for each material class are summarized in Fig. 5. In order to be conservative, the  $10 \mu\text{m}$ -fraction should be chosen as 5% for graphite and 20% for the other materials.

### Applicability of data to modelling studies

Glass is a waste immobilization matrix; grout is an encapsulation material. The break-up test data generated for these materials in the work reported here are directly applicable to assessment models. However, it should be noted that HLW glass is subject to both significant radiation fields and elevated temperatures for several years. It is currently thought that the irradiation of glass waste-forms does not alter the properties too much although there might be extra cracking. In contrast, graphite is a reactor structural material that will be subjected to irradiation, oxidizing conditions and elevated temperatures over the

TABLE 3. Mean values of the size distribution exponent  $\kappa$  in equation 5.

	$\kappa$	$\Delta\kappa$
Glass	$6.76 \times 10^{-1}$	$8.41 \times 10^{-2}$
Graphite	1.03	$3.54 \times 10^{-2}$
Grit in grout	$5.89 \times 10^{-1}$	$6.22 \times 10^{-2}$
PFA/OPC	$4.74 \times 10^{-1}$	$5.21 \times 10^{-2}$
BFS/OPC	$5.64 \times 10^{-1}$	$1.36 \times 10^{-1}$

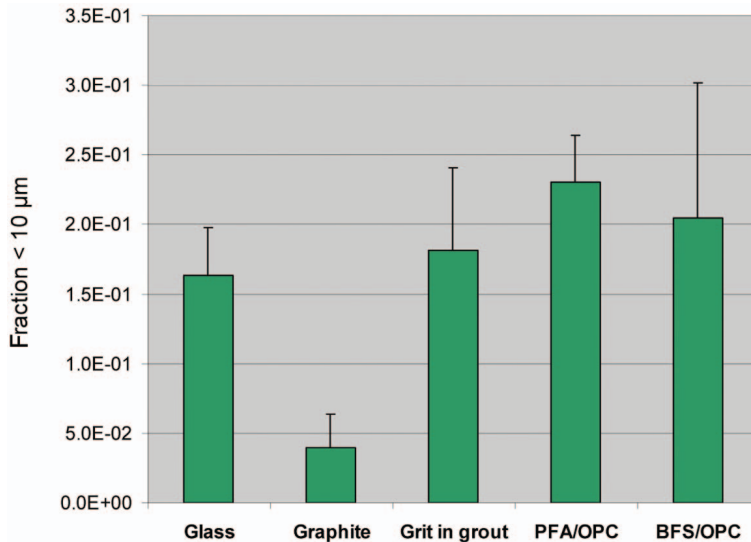


FIG. 5. Mean values of the fraction of airborne dust smaller than 10 µm.

lifetime of the plant. In this case, consideration needs to be given to the applicability of test data for as-manufactured material to that which has experienced a broad spectrum of in-service conditions.

Although mechanical property changes due to irradiation are not expected to have any significant effect upon graphite impact behaviour, microstructural changes including increased porosity may be important. Testing irradiated graphite is not an option, both because of handling issues but also because a testing programme covering a range of material conditions that could be extrapolated across a core would be too large. A more pragmatic approach would be to characterize impact behaviour using a selection of graphites covering a range of coke particle sizes and bulk porosities. The findings of such extended studies could provide a link between test data from the current study and predicted microstructural changes within a graphite core and across the Magnox fleet.

## Conclusions

In total, 136 impact tests were carried out with cylinders of various glass, graphite and grout specimens with impact speeds in the range between ~13 and 70 m s<sup>-1</sup>. The airborne release fraction (<100 µm AED) was measured in all cases, with the full size distribution in the particle

size range between 0.1 and 100 µm measured in a sub-set of experiments. The test programme has provided data describing the impact behaviour of these materials which can be used in modelling studies. However, a further programme of testing would be needed to investigate in-service ageing effects on graphite impact behaviour.

It has been shown that the airborne release fractions for the materials studied can be described by a linear expression based upon average fragmentation behaviour for each material type (glass, graphite, grout, grit in grout). Generally the relative scatter associated with the mean offset of this linear expression is quite high due to break-up statistics at low impact energies and experimental limitations for low dust emissions. The variation in the slope fitted to airborne release fraction data for all four material types is small, showing that the influence of material properties on dust formation during fragmentation of brittle materials is small.

Fragment size distributions follow a power law. Cumulative mass distributions have been evaluated for each material type based upon an aerodynamic diameter of 100 µm. In addition, fractions of airborne dust smaller than 10 µm (the respirable fraction) have been evaluated in the range 5–22% for the material types studied and conservative recommendations have been made for respirable fractions that should be used in modelling studies.



## References

- Grady, D.E. (2008) Fragment size distributions from the dynamic fragmentation of brittle solids. *International Journal of Impact Engineering*, **35**, 1557–1562.
- Lange, F., Martens, R., Nolte, O.R., Koch, W., Lödding, H. and Hörmann, E. (2003) *Improvement of the radiological and experimental basis to further develop the requirements of the IAEA transport regulations for LAS/SCO materials*. Report to the Commission of the European Communities.
- Lange, F., Martens, R., Nolte, O.R., Lödding, H., Koch, W., Hörmann, E. (2007) Testing of packages with LSA materials in very severe mechanical impact conditions with measurements of airborne release. *Packaging, Transport, Storage & Security of Radioactive Materials*, **18**, 59–71.
- Mädler, L. (1999) *Freisetzung feiner und lungengängiger Stäube durch kurzzeitige Einwirkung mechanischer Kräfte*. Unpublished PhD Thesis, TU Freiberg, Cuvillier Verlag, Göttingen, Germany.
- Meibom, A. and Baslev, I. (1996) Composite power laws in shock fragmentation. *Physical Review Letters*, **76**, 1492–1494.
- Nolte, O.R. (2005) *Determination of break-up and airborne release for different cemented materials when subject to mechanical impact for United Kingdom Nirex Limited*. Fraunhofer-ITEM Report 1129331, NDA Livelink Reference Number: 6244888.
- Nolte, O.R. (2006) *The phenomenology of fine particle formation upon fragmentation of brittle material*. Unpublished PhD Thesis, Technical University of Clausthal, Clausthal, Germany, [in German].
- Oddershede, L., Dimon, P. and Bohr, J. (1993) Self-organized criticality in fragmentation. *Physical Review Letters*, **71**, 3108–3110.